J. of Active and Passive Electronic Devices, Vol. 2, pp. 93–103
Reprints available directly from the publisher
Photocopying permitted by license only

Tribological behavior of chromium nitride coating by unbalanced magnetron sputtering

S. M. MUSAMEH*, S.W. JODEH

Physics Department, An – Najah University, Nablus, P.O. Box 7. West Bank, Palestine
Chemistry Department, An – Najah University, Nablus, P.O. Box 7 West Bank, Palestine

The possibility of improving tribological properties of aluminum alloys using a chrome nitride coating is exploded. Thin films of Cr_xN_{1-x} were deposited on aluminum 6061 using a reactive sputtering technique in an unbalanced magnetron deposition system. The structure, composition, and morphology of the deposited thin films were characterized by using x-ray diffraction (XRD), scanning electron microscopy (SEM), electron – probe microanalysis (EPMA), and x-ray photoelectron spectroscopy (XPS).

Key words: Chromium nitride; coating; magnetron sputtering; and aluminum alloys

INTRODUCTION

Aluminum alloys have become increasingly important to be used in reducing the weight of automobiles. While aluminum alloys have high strength – to – weight ratio, they usually have poorer resistance than that of iron and steel based materials [1–4]. There are many research activities to improve the tribological properties of aluminum alloys, such as applying various surface coatings produced by thermal spray [3–7], pulsed laser deposition (PLD), electrochemical micro vapor deposition [8–16], and ion implantation [17–23]. There has been interest in applying various surface coatings to the molding dies in order to reduce the coefficient of friction [24, 25], extend die life [26] and also to protect functional molding components of aluminum alloys such as erosion, corrosion, creep and thermal fatigue [12, 13, 27–28]

* Corresponding Author: E-mail: musameh@najah.edu or to shms10@yahoo.com

In the present paper, fundamental tribological, the growth, structure, and mechanical property of Cr_xN_{1-x} thin films on an aluminum alloy surface are described in detail.

Chromium nitride (CrN) was chosen because of its thermal resistance, high hardness, low internal stress, corrosion resistance and most importantly, ease of mold release [1–13]. CrN has a variety of applications such as automobile power train subsystem [19, 20], machining tools [13, 21], replacement for electroplated Cr [21, 22] and dry-cutting [23].

EXPERIMENTAL PROCESS

Aluminum 6061 T6 rod of 24.5 cm diameter was used to get the samples in a form of disks from the rod, the aluminum disks were polished using 1-u diamond paste, then they were thorough wet cleaned in an ultrasonic bath before being loaded into Unbalanced Magnetron Sputtering System (UMSS) for Cr_xN_{1-x} as shown in Fig. 1. Single crystal Si wafers with approximately 100 nm SiO_2 coating were also used as substrates for each film deposition. The Si wafers and the aluminum alloy disks were subjected to Ar^+ bombardment at -400 V bias voltages to ensure good adhesion and clean deposited films from any oxides.

The Cr_xN_{1-x} coatings thin films were deposited by using chromium from two targets of 99.99% in pure nitrogen–containing argon environment, the pressure during deposition stage was kept at 0.13Pa. The nitrogen flow rate was varied between 10 and 75 slandered cubic centimeters (sccm) to provide different ratio of Cr/N thin films, the Cr_xN_{1-x} films were deposited at 4 amperes with -60 V bias applied to the substrate, which was kept at temperature below 180° C.

The structure of the thin film was studied by x-ray diffraction (XRD) using Siemens D5000 diffractometer configured in parallel beam geometry with Cu Kα radiation. The diffractometer is equipped with a Gobel mirror and a LiF (100) monochromatic. Data was collected from 33 to 70 degrees two theta at 10 sec/step, 0.05 degrees/step and a fixed incidence angle of 2 degrees. The surface morphology was examined using a Hitachi S4000 scanning electron microscope (SEM). The composition of the films was determined quantitatively by electron probe microscope (EPMA) using a camera model SX100 to determine the Cr/N ratio, each film had a 100–nm interlayer of chromium to promote adhesion. The thickness of the Cr_xN_{1-x} layer was measured by using a Philtec radial sectioning system.

The heterogeneity of the films (composition vs. depth) and the presence of impurities, such as oxygen, were determined using x-ray photoelectron

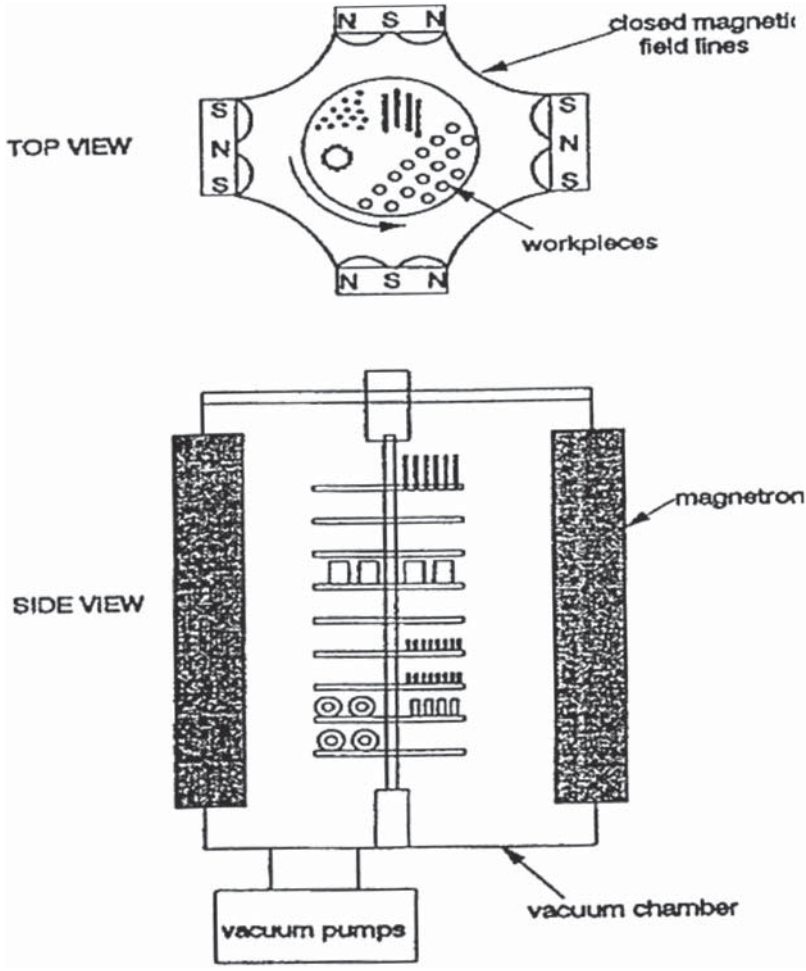

FIGURE 1
Schematic diagram of the unbalanced magnetron deposition system.

spectroscopy (XPS) combined with Ar-ion sputtering. A Surface Science Instruments Model SSX-101 M-Probe spectrometer was used.

Cross - section and microstructure observations of the deposited films were Measured using scanning electron microscopy (SEM; Hitachi S4000) and X– ray diffractometry (XRD; Siemens D5000). The tribological tests of CrN coatings were performed on a ball–on-disc tribometer (ISC–200) with no lubricant.

TABLE 1

Sample Name	Nitrogen Flow (sccm)	at. % Cr	at. % N	Cr/N
CrN100	0	100	0	—
CrN90	5	100	0	—
CrN80	10	85	15	5.67
CrN65	16	69	31	2.23
CrN50	25	53	47	1.13
CrN35	46	51	49	1.04
CrN20	75	52	48	1.09

RESULTS AND DISCUSSIONS

Film Composition and Structure Analysis

Electron probe microanalysis (EPMA) was used to determine the composition of the films and the results are summarized in table 1. As the N_2 flows rate increasing, the Cr to nitrogen ratio decreases. The Cr/N ratio reaches a constant (1) value when there is sufficient supply of N_2. Fig. 2. Indicates the formation of CrN phase, which exist over a narrow range of composition according to the equilibrium phase diagram.

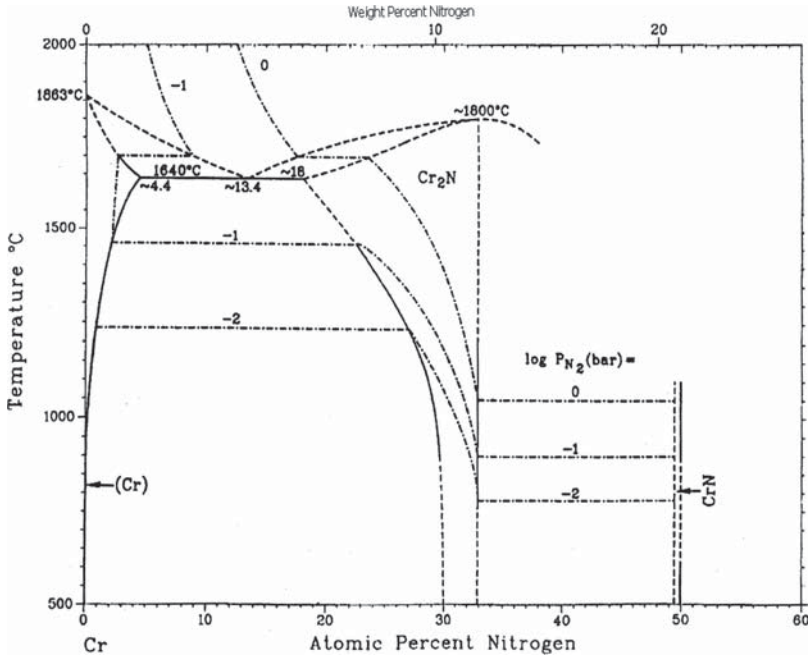

FIGURE 2
Phase diagram for chromium nitride.

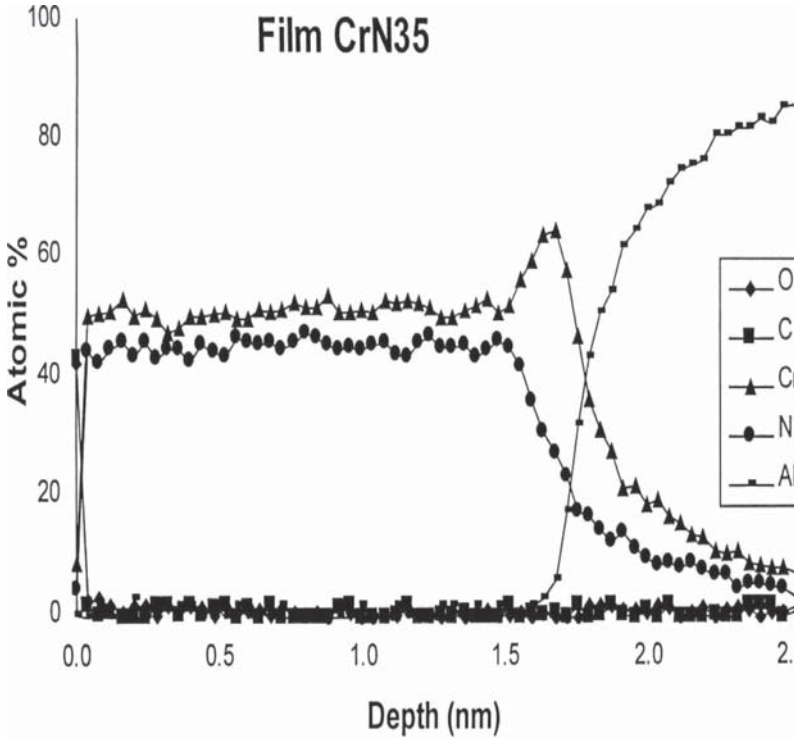

FIGURE 3
XPS depth profile of CrN35 showing the contaminant–free CrN and the Cr interlayer on the aluminum substrate.

Composition depth profiles and impurity levels were obtained using XPS together with 4-kV Ar+ sputtering. The concentration of Cr and N were homogeneous in the bulk of the coating. Carbon and oxygen impurity levels in films Cr100, CrN80, and CrN35 were below the detection limit of approximately 1.0 at %. The interface between the coating and the aluminum alloy substrate was also free of oxygen and carbon impurities, indicating that the sputter-cleaning step was effective in removing contaminants and native oxides from the aluminum alloy surfaces. A typical depth profile of Cr_xN_{1-x} coated aluminum 6061 (sample CrN35) is showing in figure 3.

The x-ray diffraction (XRD) patterns typical of the samples are shown in figure 4. The sharp diffraction peaks are from the aluminum 6061 substrate. The variation in the intensity of the aluminum diffraction peaks is a result of variations in the coating thickness. The three samples with the largest nitrogen concentration (CrN20, CrN35, CrN50) are similar. The CrN35 and CrN50 peaks match those of CrN given in the JCPDS database (No. 11–65) as in reference [25], the CrN peak position are at a lower

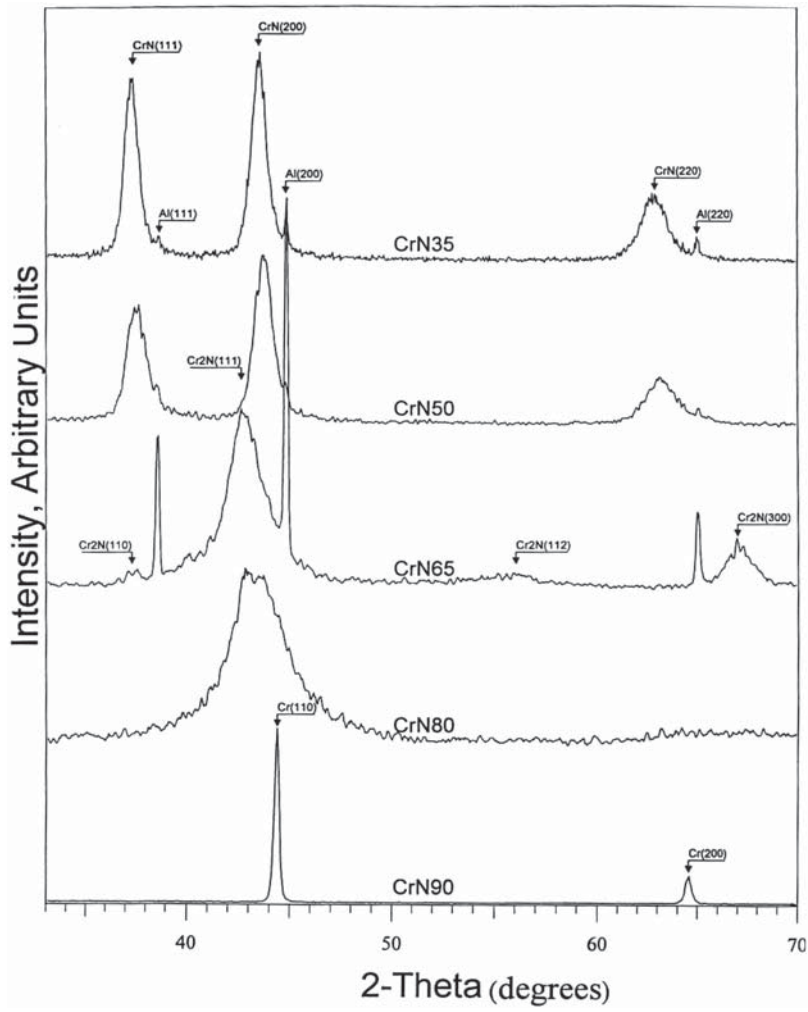

FIGURE 4
X-ray diffraction pattern for all CrN films.

diffraction angles than the JCPDS reference. From the CrN (111), (200) and (220) peak positions, the lattice parameters are 4.183 Å, 4.180 Å, and 4.157 Å from samples CrN20, CrN35 and CrN50, respectively. Comparing with the reference value of 4.140 Å, the lattice parameter of the films is about 1.4% larger [25].

Samples CrN20 differ from CrN35 and CrN50 in the relative intensities of the CrN (111) and (200) diffraction peaks. This difference is attributed to differences in the crystal texture. The relative intensities of CrN diffraction

peaks for sample CrN20 also deviate from those given in the JCPDS reference, while samples CrN35 and CrN50 have a more random crystal texture.

Differences in CrN peak broadening were also observed between these three samples. Using the Scherrer equation [26], and the full-width half-maximum of the CrN (111), (200) and (220) diffraction peaks, the crystal size for the samples are, assuming the peak broadening is caused by crystal size, 140 Å, 110 Å, and 80 Å for samples CrN20, CrN35 and CrN50, respectively.

The diffraction data for sample CrN65 matches JCPDS reference data [25], for Cr_2N (No. 35803). Lattice parameter calculated from the Cr_2N (110), (111), (112) and (300) peak positions ($a = 4.824$ Å, $c = 4.509$ Å) were slightly larger than the JCPDS reference ($a = 4.811$ Å and $c = 4.484$ Å). This corresponds to a lattice parameter expansion of 0.27% and 0.56% in a- and c-dimensions, respectively. Using

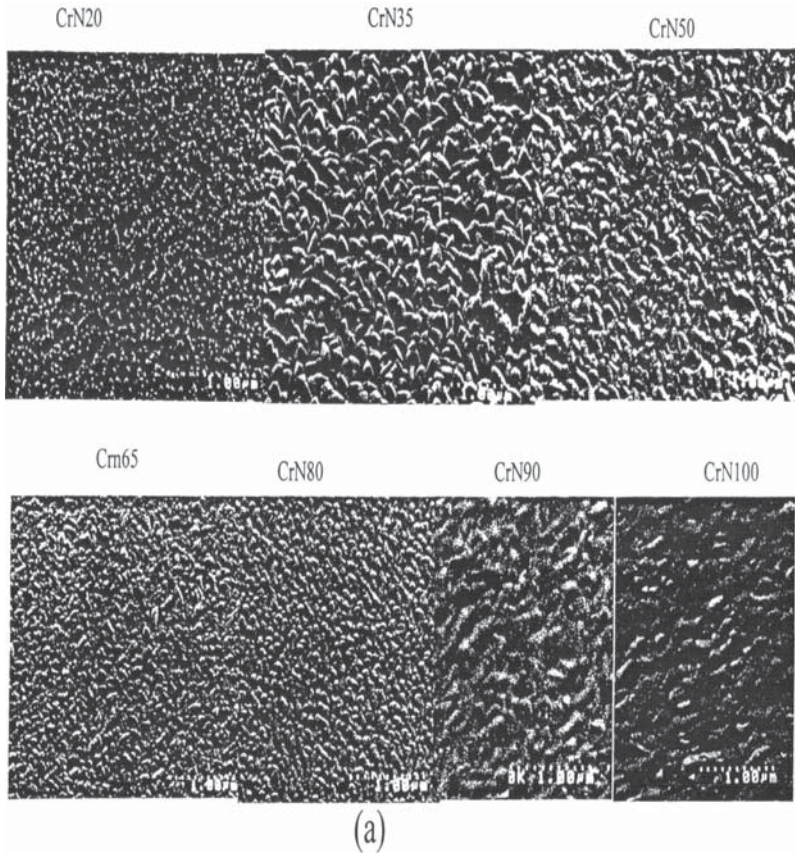

FIGURE 5
SEM photos of top view (a) and cross section (b) of all the CrxNr-x film.

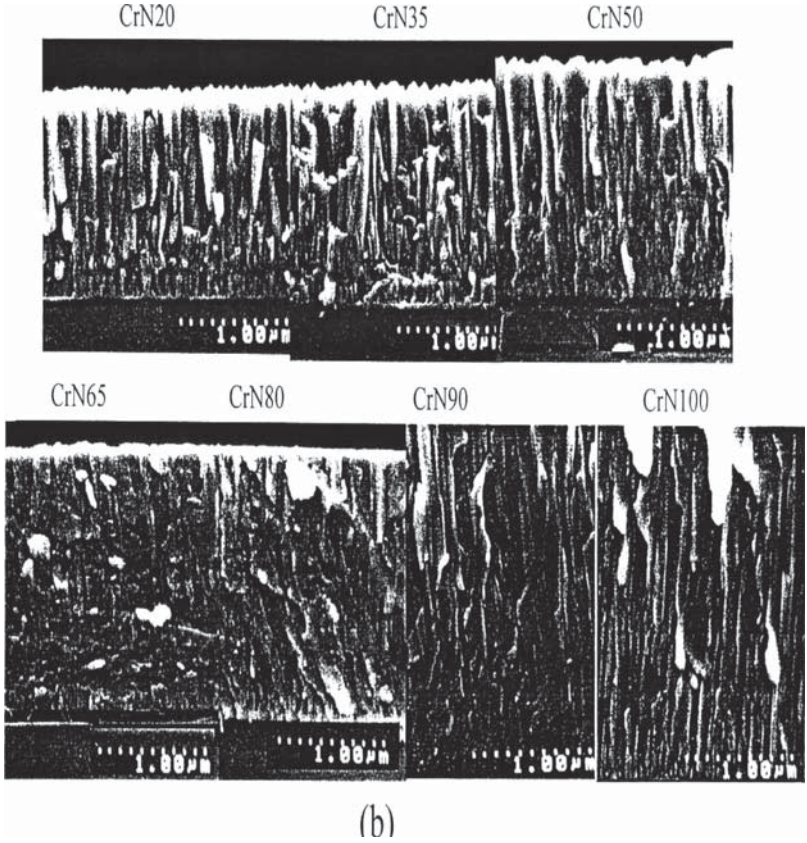

FIGURE 5
(*cont.*)

the Scherrer equation and the full-width half-maximum of the Cr_2N (110), (111), (112) and (300) diffraction peaks, the average crystal size was estimated to be 70 Å.

The diffraction data for sample CrN80 had a broad diffraction peak at about 44.5° two theta. The slight splitting at the peak indicates this film is a mixture of two phases. The displacing of the doublet (2.800 Å and 2.113 Å), along with the low nitrogen concentrations, suggest that this sample is a mixture of Cr and Cr_2N with the diffraction peaks attributes to the Cr 9 110) and Cr_2N (111) reflections. Using the Scherrer equation and the full-width half-maximum calculated from the dis-consolation of the doublet, the crystal size was estimated at 30 Å for the Cr phase and 120 Å for Cr_2N phase. Thus, the film is nanocomposite consisting of Cr and Cr_2N.

The diffraction data for sample CrN90 and CrN100, shown in figure 4, Match JCPDS reference data for Cr (No. 6–694). 25 the lattice parameter calculated from the Cr (110) and (200) peak position was 2.889 Å for both samples and was nearly identical to the JCPDS reference value of 2.884 Å.

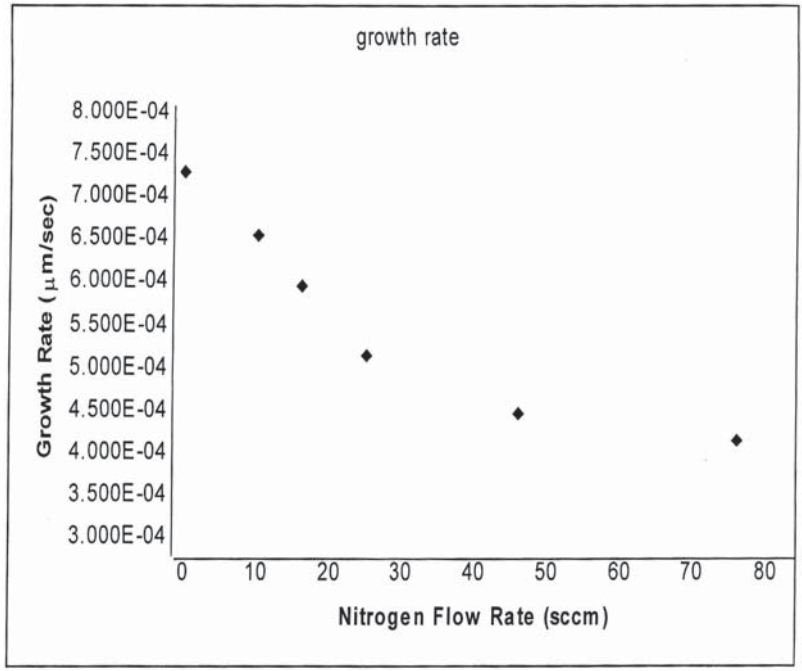

FIGURE 6
Deposition as a function of N_2 flow rate.

Form the lattice parameter calculation, it can be assumed no nitrogen was incorporated into the chromium lattice. The diffraction peaks from both CrN90 and CrN100 were the sharpest. Using the Scherrer equation and the full-width half maximum of the Cr (110) and (200) diffraction peaks, the average crystal size was estimated to be 250 Å for both CrN90 and CrN100 samples.

CONCLUSIONS

In this paper thin films of Cr_xN_{1-x} were deposited on the surface of aluminum 6061 using an unbalanced magnetron sputtering technique. The original points are:

The composition of the films is uniform, the film and the interface between Cr_xN_{1-x} and the substrate are free from carbon and oxygen contaminants. This ensures good coating adhesion.

Pure Cr, Cr_2N and CrN phase can form by varying the composition of sputtering gas. The highest hardness was found in film consisting of

Cr, Cr_2N phases. The hardness and elastic modulus depend strongly on the composition and structure Cr_xN_{1-x} of the coating.

We have shown that using the technique of a chrome nitride (CrN) coating will help in investigating and improving the tribological properties of aluminum alloys, which can be used for automobile engine applications.

ACKNOWLEDGMENTS

The authors wish to acknowledge the GM and university of Windsor for letting them to use their lab and also Dr. Musameh wants to thank Najah - university for partially support this work by giving him a sabbatical leave.

REFERENCES

[1] P. A. Deamly. (1999). *Wear., 1109,* 225–229.

[2] K. Nakata. (1997). *Japanese Journal of Tribology, 42,* 195–198.

[3] D. Heim, F. Holler, and C. Mitterer. (1999). *Surf. Coat. Tech., 116/119,* 530.

[4] K. T. Rie, C. Pfohl, C. H. Lee, and C. S. Kang. (1999). *Surf. Coat. Tech., 97,* 232.

[5] E. J. Bienk, H. Reitz, and N. J. Mikkelson. (1995). *Surf. Coat. Tech., 76–77,* 475–480.

[6] Y. K. Wang, L. Sheng, R. Z. Xiong, and B. S. Li. (1999). *Surface Engineering, 15,* 109.

[7] E. Lugscheider, G. Krämar, C. Barimani, and H. Zimmermann. (1995). *Surf. Coatings Tech., 74–75,* 497.

[8] J. Senf, and E. Broszeit. (1999). *Mat. -Wiss.u. Werkstofftech, 30,* 262.

[9] P. Hedenqvist, S. Jacobson, and S. Hogmark. (1997). *Surf. Coat. Tech., 97,* 656–660.

[10] K. C. Walter, J. T. Scheuer, P. C. McIntyre, P. Kodali, N. Yu, and M. Nastasi. (1996). *Surf. Coat. Technol., 85,* 1.

[11] D. Y. Wang, and M. J. Chiu. (2001). *Surf. Coat. Technol., 137,* 164.

[12] W. Y. Ho, D. H. Huang, L. T. Huang, C. H. Hsu, and D. Y. Wang. (2004). *Surf. Coat. Tech., 177–178,* 172–177.

[13] M. Uchida, N. Nihira, A. Mitsuo, K. Toyoda, K. Kubota, and T. Aizawa. (2004). *Surf. Coat. Tech., 177–178,* 627–630.

[14] C. S. Lin, C. S. Ke, and H. Peng. (2001). *Surf. Coat. Techol., 146–147,* 168.

[15] A. Molinari, M. Pellizzari, G. Straffelini, and M. Pirovano. (2000). *Surf. Coat. Technol., 126,* 31.

[16] S. C. Lee, W. Y. Ho, and F. D. Lai. (1996). *Mater. Chem. Phys., 43,* 266.

[17] A. Persson, J. Bergström, C. Burman, and S. Hogmark. (2001). *Surf. Coat. Technol., 146–147,* 42.

[18] M. A. M. Ibrahim, S. F. Korablov, and M. Yoshimura. (2002). *Corros. Sci., 44,* 815.

[19] M. Kano, T. Sakane, and M. Matsuura. (1996). *Japanese J. Tribology., 42,* 1021.

[20] E. Broszeit, C. Friedrich, and G. Berg. (1999). *Surf. Coatings Tech., 115,* 9.

[21] B. Navinšek, P. Panjan, and I. Milošev. (1997). *Surf. Coatings Tech., 97,* 182.

[22] J. Stockemer, R. Winand, and P. V. Brande. (1999). *Surf. Coatings Tech., 115,* 230.

[23] E. Lugscheider, O. Knotek, C. Barimani, T. Leyendecker, O. Lemmer, and R. Wenke. (1995). *Surf. Coatings. Tech., 74–75,* 497.

[24] X. M. He, N. Baker, B. A. Kehler, K. C. Walter, and M. N. Nastasi. (2000). *J. Vac. Sci. Tech., A18,* 30.

[25] P. Panjan, P. Cvahte, M. Cekada, and B. Navinšek. (2001). *UrankarI., Vacuum, 61,* 168.

[26] C. Meunier, S. ViVes, and G. Bertrand. (1998). *Surf. Coatings Tech., 107,* 149.

[27] Y. Jin, and Y. Yang. (1996). *Surf. Coat. Technol., 88,* 248.

[28] J. Almer, M. Odén, and L. Hultman. (2000). *J. Vac. Sci. Tech., A18,* 121.